ResearchGate

See discussions, stats, and author profiles for this publication at: https://www.researchgate.net/publication/45661562

Probing the Peptidylglycine α-Hydroxylating Monooxygenase Active Site with Novel 4-Phenyl-3-butenoic Acid Based Inhibitors

ARTICLE *in* CHEMMEDCHEM · SEPTEMBER 2010

Impact Factor: 2.97 · DOI: 10.1002/cmdc.201000214 · Source: PubMed

CITATIONS
4

READS
15

8 AUTHORS, INCLUDING:

Marius Réglier
French National Centre for Scientific Resea…
103 PUBLICATIONS **1,315** CITATIONS
SEE PROFILE

Michele Saviano
Italian National Research Council
248 PUBLICATIONS **3,005** CITATIONS
SEE PROFILE

Luciana Esposito
Italian National Research Council
39 PUBLICATIONS **784** CITATIONS
SEE PROFILE

Renaud Hardré
Aix-Marseille Université
34 PUBLICATIONS **468** CITATIONS
SEE PROFILE

Available from: Luciana Esposito
Retrieved on: 24 January 2016

CHEMMEDCHEM

DOI: 10.1002/cmdc.201000214

Probing the Peptidylglycine α-Hydroxylating Monooxygenase Active Site with Novel 4-Phenyl-3-butenoic Acid Based Inhibitors

Emma Langella,[a] Sébastien Pierre,[b] Wadih Ghattas,[b] Michel Giorgi,[c] Marius Réglier,*[b] Michele Saviano,[a] Luciana Esposito,*[a] and Renaud Hardré[b]

Specific inhibition of the copper-containing peptidylglycine α-hydroxylating monooxygenase (PHM), which catalyzes the post-translational modification of peptides involved in carcinogenesis and tumor progression, constitutes a new approach for combating cancer. We carried out a structure–activity study of new compounds derived from a well-known PHM substrate analogue, the olefinic compound 4-phenyl-3-butenoic acid (PBA). We designed, synthesized, and tested various PBA derivatives both in vitro and in silico. We show that it is possible to increase PBA affinity for PHM by appropriate functionalization of its aromatic nucleus. Compound **2d**, for example, bears a *meta*-benzyloxy substituent, and exhibits better inhibition features ($K_i = 3.9$ μM, $k_{inact}/K_i = 427\ M^{-1}s^{-1}$) than the parent PBA ($K_i = 19$ μM, $k_{inact}/K_i = 82\ M^{-1}s^{-1}$). Docking calculations also suggest two different binding modes for PBA derivatives; these results will aid in the development of further PHM inhibitors with improved features.

Introduction

C-terminal glycine-extended peptide amidation is a post-translational modification involved in the biosynthesis of certain neuropeptides and peptide hormones such as substance P, oxytocin, neuropeptide Y, and adrenomedullin. Peptide amidation is catalyzed by the bifunctional enzyme peptidylglycine α-amidating monooxygenase (PAM, EC 1.14.17.3), which possesses two different catalytic domains: the peptidylglycine α-hydroxylating monooxygenase (PHM) domain and the peptidyl-α-hydroxyglycine α-amidating lyase (PAL) domain. The copper-, ascorbate-, and dioxygen-dependent PHM domain catalyzes the hydroxylation of C-terminal glycine residues to form hydroxyglycine, which is then transformed into an amidopeptide and glyoxylic acid by the PAL domain (Scheme 1).[1]

The PHM structure consists of two domains, each of which contains one copper atom and is essentially composed of a β sandwich formed by two β sheets.[2–5] The two copper centers are ~11 Å apart, separated by a solvent-filled cavity. They are not functionally equivalent: one copper atom (Cu_M) binds O_2, and hydroxylation of the bound substrate occurs at this site, whereas the other copper atom (Cu_H) is involved only in electron transfer. The Cu_M atom is tetrahedrally coordinated by two histidine residues and one methionine, with the fourth position occupied by O_2 or a water molecule.[2–5] The Cu_H atom is ligated by three histidine residues in a T-shaped coordination geometry. The structural features of PHM and its active site in particular have been elucidated by crystallographic characterization of multiple forms of the enzyme, including reduced and oxidized PHM (PDB IDs: 3PHM[3] and 1PHM,[2] respectively) as well as an oxidized form with bound substrate (1OPM[3]), a reduced form with bound slow substrate and O_2 (1SDW[4]), and four structures of a new crystal form of the enzyme (1YIP and 1YJK, the respective oxidized and reduced new PHM forms, and 1YI9 and 1YJL, the oxidized and reduced M314I mutant forms, respectively).[5]

The reduced and oxidized forms of the enzyme—with or without bound substrate—are very similar (RMSD = 0.3 Å at Cα atoms) both in the conformations of individual residues and in the overall structure, indicating that there is no inter-domain

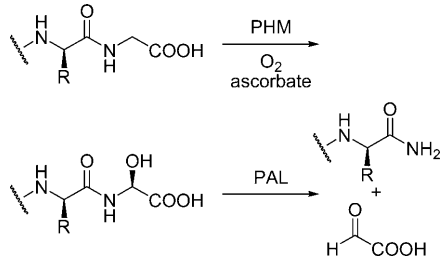

Scheme 1. PAM-catalyzed reactions.

[a] *Dr. E. Langella, Dr. M. Saviano, Dr. L. Esposito*
Istituto di Biostrutture e Bioimmagini, CNR
via Mezzocannone 16, 80134 Napoli (Italy)
Fax: (+39) 081-253-4574
E-mail: luciana.esposito@unina.it

[b] *Dr. S. Pierre, Dr. W. Ghattas, Dr. M. Réglier, Dr. R. Hardré*
Institut des Sciences Moléculaires de Marseille, équipe BiosCiences
UMR-CNRS 6263, Aix-Marseille Université
av. Escadrille Normandie-Niemen, 13397 Marseille Cedex 20 (France)
Fax: (+33) 4-9128-8440
E-mail: marius.reglier@univ-cezanne.fr

[c] *Dr. M. Giorgi*
Spectropole, FR1739-CNRS, Aix-Marseille Université
av. Escadrille Normandie-Niemen, 13397 Marseille Cedex 20 (France)

Supporting information for this article is available on the WWW under http://dx.doi.org/10.1002/cmdc.201000214.

View this journal online at wileyonlinelibrary.com

© 2010 Wiley-VCH Verlag GmbH & Co. KGaA, Weinheim

movement or significant structural reorganization during the reaction cycle.[4] The substrate binding site has been accurately described by analyzing the oxidized structures containing either *N*-α-acetyl-3,5-diiodotyrosylglycine (IYG)[3] or *N*-α-acetyl-3,5-diiodotyrosylthreonine (IYT).[4] The Cα atom of glycine, where the stereospecific abstraction of hydrogen occurs, is positioned ~4 Å away from Cu_M, proximal to the fourth coordination position of Cu_M, the O_2 coordination site.

Amidopeptides resulting from PAM modification act as neurotransmitters and hormones, and aberrancies in their regulation are involved in numerous diseases.[6] Adrenomedullin (AM), a 52-residue amidopeptide, is implicated as a mediator of several pathologies such as cardiovascular and renal disorders, sepsis, inflammation, diabetes, and cancer.[7] Findings over the past few years have implicated AM as a major regulator of carcinogenesis and tumor progression and have identified it as a putative target in the development of new cancer treatment strategies. Rocchi et al. demonstrated high expression levels of PAM and AM in hormone-independent prostate cancer specimens,[8] indicating that AM plays a key role in the proliferation of such cancers. Moreover, the use of specific anti-AM antibodies proved effective in the treatment of mice carrying human glioblastoma.[9] Given that AM is inactive without C-terminal amidation, the inhibition of PAM in the tissue of interest would constitute a new strategy in the development of therapies against hormone-independent prostate cancer and possibly other types of cancer.[10]

Intense efforts have been made to find effective PHM inhibitors.[11,12] Despite the debate concerning the potential toxicity of an anti-PHM drug, some compounds have been shown to block the proliferation of cancer cells.[13] The applicability of such compounds could be stimulated by the continued development of efficient and selective PHM inhibitors in concert with effective delivery systems to target cancer cells specifically.

In this context, we carried out a structure–activity study of new compounds derived from a well-known PHM substrate analogue, the olefinic compound 4-phenyl-3-butenoic acid (PBA).[14] Independent studies performed both in vitro[15] and in vivo[16] have revealed that PBA is a potent PHM inhibitor. Although no covalent adduct was observed,[15] PBA exhibits features of mechanism-based inhibition,[17,18] and it is believed that inhibition occurs through the formation of a delocalized radical (Scheme 2). Given that AM contains a tyrosine residue at the penultimate position, we used the aromatic ring of PBA as a platform for positioning the aromatic nucleus in order to mimic this tyrosine residue. Herein we report the synthesis and in vitro and in silico activity of new functionalized PBA derivatives containing methyl, methoxy, and benzyloxy substituents at the *meta* and *para* positions of the aromatic ring (Scheme 3).

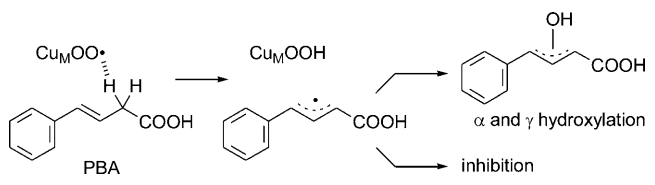

Scheme 2. Mechanism-based inhibition of PHM by PBA, suggesting the occurrence of a delocalized radical.[15]

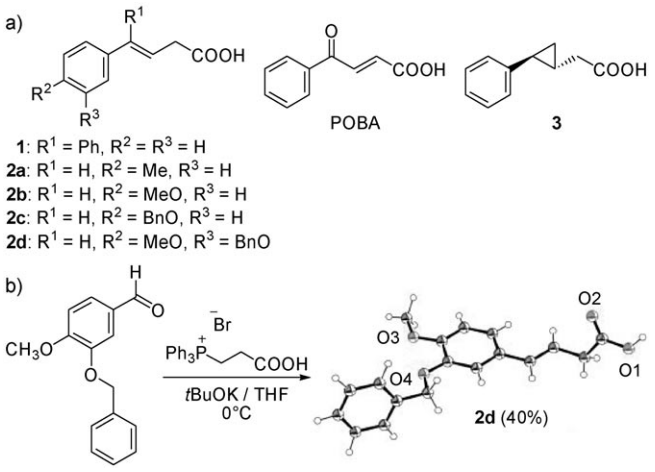

Scheme 3. a) PBA derivatives tested; b) synthesis and ORTEP view of derivative **2d**.

Results

Syntheses

Compounds **1**,[19] **2a**,[20] **2b**,[21] and **3**[22] were prepared by published procedures. The new PBA derivatives **2c** and **2d** were synthesized by Wittig reaction between 2-carboxyethyltriphenylphosphonium bromide and the corresponding aldehydes. Recrystallization of compound **2d** in acetonitrile afforded crystals suitable for X-ray diffraction analysis (CCDC 735325; Scheme 3).

Inhibition

PHM is present in soluble and membrane-bound forms. Given that both forms share the same kinetic features,[14] experiments were conducted with the membrane-bound form of porcine PAM obtained from pig left atria which is readily available in our laboratory. Incubation of PAM at 37 °C in air with various concentrations of compounds **1**–**3** (at least five concentrations in the range of 0–10 μM) resulted in a time-dependent loss of enzyme activity (Figure 1). As a reference, we also monitored the activity of the well-characterized PHM inhibitors PBA[14] and POBA.[23] The rate of activity loss was determined by taking aliquots and measuring the residual activity by HPLC with *N*-dansyl-D-Tyr-L-Val-Gly as substrate.

Under our experimental conditions with porcine PAM, PBA and POBA exhibited kinetic features that are consistent with published data.[14,23] Except for compounds **1** and **3**, which are not efficient inhibitors, PBA derivatives **2a**–**d** show efficiencies equal to higher than that of the parent compound PBA (Table 1). For example, compound **2d**, which bears a *meta*-benzyloxy substituent, exhibits better inhibition features (K_i = 3.9 μM, k_{inact}/K_i = 427 $M^{-1}s^{-1}$) than the parent PBA (K_i = 19 μM,

 © 2010 Wiley-VCH Verlag GmbH & Co. KGaA, Weinheim

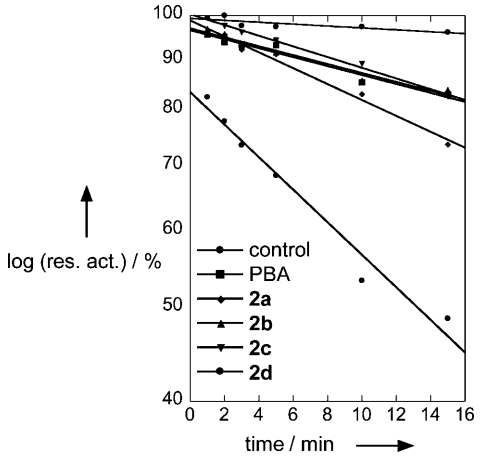

Figure 1. Comparative time-dependent inactivation of porcine PAM by PBA derivatives **2a**–**d** at 2.5 μM. The residual activities were determined by taking aliquots and measuring the activity by HPLC with *N*-dansyl-D-Tyr-L-Val-Gly as substrate (the full set of kinetic data is given in figures 1–6 in the Supporting Information).

Table 1. Measured and calculated inhibition kinetics parameters for PHM by PBA derivatives.

Compd	K_i [μM][a]	k_{inact} [min^{-1}]	k_{inact}/K_i [$M^{-1}s^{-1}$]	K_i^{calcd} [μM][b] COO^-/R240
PBA[c]	19±2	0.094±0.006	82±14	27.6
POBA[d]	440±50	0.15±0.02	6±1	ND
1	>700	ND	ND	38.9
2a	5.7±0.9	0.062±0.006	181±33	28.9
2b	15±2	0.07±0.02	60±7	ND
2c	19±2	0.10±0.03	88±5	ND
2d	3.9±0.7	0.10±0.01	427±41	4.1
3	131±26	0.028±0.003	4±1	51.1

[a] Measured on porcine PHM. [b] Calculated K_i values determined by docking with rat PHM; only the COO^-/R240 binding mode is reported, as it is the only one compatible with the suicide inhibition mechanism suggested for these inhibitor experiments. [c] For rat PHM, K_i=47 μM and k_{inact}=0.29 min^{-1}.[14] [d] For rat PHM, K_i=160 μM and k_{inact}=3.6 min^{-1}.[23]

k_{inact}/K_i=82 $M^{-1}s^{-1}$). In all cases, the loss of activity was correlated to the concentration of inhibitor. By plotting the reciprocal rate of inactivation as a function of the reciprocal of the inhibitor concentration according to the method of Kitz and Wilson,[24] $1/k_{inact}$ and $-1/K_i$ constants were obtained as *y*- and *x*-intercepts, respectively. These data as well as the k_{inact}/K_i ratio are listed in Table 1.

We observed that compounds **2a**–**d** fulfill the minimal criteria for mechanism-based ("suicide") inhibitors:[17,18] 1) The inactivation is time dependent (Figure 1). 2) The inactivation is also O_2 and ascorbate dependent; when incubations were performed in degassed solution or in the absence of reducing agent, inactivation was not observed (Table 2). 3) Inactivation is prevented in the presence of substrate; *N*-dansyl-D-Tyr-L-Val-Gly (50 μM) at 20-fold molar excess over PBA derivatives (2.5 μM) blocked PHM inactivation (Table 2). 4) Inactivation is not reversed after extensive dialysis; the 15 min incubation mixture was subjected to dialysis against MES buffer (pH 6.5, 100 mM), and the activity was measured after reconstitution with $CuSO_4$ (2 μM) for 1 h in MES buffer (pH 6.5, 100 mM) at 4 °C. In all cases, the same level of inactivation was observed. We determined that under the same conditions, active PHM retains >95% of its initial activity.

Table 2. The role of cofactors in the time-dependent inactivation of porcine PHM by PBA derivatives **2a**–**d**.[a]

PBA	Reaction Components			Res. Act. [%][c]	
	O_2 (250 μM)	Ascorbate (10 mM)	Substrate (50 μM)[b]	5 min	15 min[d]
2a	+	+	–	91	74 (70)
	+	+	+	96	96
	+	–	–	98	97
	–	+	–	97	99
2b	+	+	–	91	84 (77)
	+	+	+	97	98
	+	–	–	96	97
	–	+	–	98	95
2c	+	+	–	94	82 (75)
	+	+	+	99	97
	+	–	–	96	98
	–	+	–	97	97
2d	+	+	–	68	49 (45)
	+	+	+	95	96
	+	–	–	98	97
	–	+	–	98	99

[a] Incubations with PBA derivatives (2.5 μM) and the indicated variables were carried out at 37 °C in MES buffer (pH 6.5, 100 mM) containing NEM (500 μM), $CuSO_4$ (2 μM), and catalase (6500 U). [b] *N*-dansyl-D-Tyr-L-Val-Gly. [c] The residual activities at 5 and 15 min were determined by taking aliquots and measuring the activity by HPLC with *N*-dansyl-D-Tyr-L-Val-Gly as substrate. [d] In brackets: values after dialysis and 1 h reconstitution with $CuSO_4$ (2 μM) in MES buffer (pH 6.5, 100 mM) at 4 °C.

Docking

A docking analysis was performed with the AutoDock program[25] to assess the putative binding mode of the experimentally characterized inhibitors and to understand the ligand–protein interactions in detail. In particular, the computational analysis was focused on PBA and on some representative compounds that exhibit different inhibition affinities toward PHM. A key step in the docking analysis was the assessment of the docking protocol. Our early attempts to perform docking calculations for the PBA derivatives by keeping the atomic coordinates of the receptor fixed were negatively affected by the position of the long side chain of K134. This Lys residue is located at the mouth of the inter-domain crevice near the active site, with the Nζ atom directed toward the oxygen atom of T132. Indeed, the positively charged side chain of K134 prevents our compounds from exploring the whole protein cavity in the vicinity of the active site. In contrast, examination of the available X-ray crystal structures of rat PHM both in the reduced and oxidized states reveals that the side chain of K134 has consistently high *B* factors and can also adopt various conformations.[2–5] This indicates that the side chain is flexible; there-

 © 2010 Wiley-VCH Verlag GmbH & Co. KGaA, Weinheim

fore, its position in the X-ray structure could introduce artifacts into docking calculations, which consider the protein as a rigid entity. To minimize this potential bias coming from the experimental structure, we carried out calculations including the flexibility of the K134 side chain. We also tested the flexibility of other amino acids within the active site (Y318, N316, and R240, involved in IYG binding) alone or together, but we could not obtain better results than those with the rigid docking, and so we kept them inflexible in our calculations.

The docking protocol was validated for the oxidized rat structure (PDB ID: 1OPM[3]) by predicting the binding mode of the bound substrate IYG, for which the experimental affinity constant is known ($K_i = 3$ μM). The IYG molecule was removed from the active site and docked back into the protein, either with or without taking into account the flexibility of K134. AutoDock successfully predicted the binding mode of IYG in both cases, and the results reported hereafter refer to the flexible docking analysis. Indeed, the best-ranked conformation from AutoDock was very close (RMSD = 1.3 Å on all atoms) to the experimentally determined position in the crystal structure (Figure 2a). Indeed, all the major interactions between the ligand and the receptor are conserved. The IYG carboxylate group forms a hydrogen bond with Y318 and a bidentate salt bridge to the guanidinium group of R240. The IYG amide NH group of glycine is hydrogen bonded to the side chain of N316. The diiodotyrosine side chain is accommodated in a loose hydrophobic pocket displaying van der Waals (vdW) interactions mainly with M208 and L206. The calculated binding constant ($K_i = 5.8$ μM) is also similar to the experimental value.

Once the procedure was established, we docked the PBA molecule into the active site. The docked compound shows two mainly populated conformations characterized by different anchoring points for the carboxylate group of the ligand: the positively charged side chains of either K134 or R204. The lower-energy and more populated of the two clusters of conformations is represented by orientations involving the binding to R240 (Figure 2b), as observed for the substrate in the IYG–PHM complex. The aromatic ring of PBA occupies a position slightly different from that found in the X-ray complex. Indeed, the ring and the olefinic moieties are pushed deeper into the crevice, displaying vdW contacts with hydrophobic residues (Y318, F112, I137, all within 3.5 Å; L206, and K134, within 4 Å). In the representative conformation of this cluster, the distance between the catalytic Cu_M center and the ligand methylene C atom is ~5.8 Å. This value is similar to that found in the experimental structure where the corresponding distance between Cu_M and the Gly Cα atom in IYG is 4.3 Å. Also, the native interaction between the ligand carboxylate and Y318 Oη is preserved in this orientation. The estimated inhibition constant K_i is 27.6 μM, close to the experimentally observed value of 19 μM (Table 1).

The second most populated cluster corresponds to a conformation in which the ligand carboxylate group is engaged in an electrostatic interaction with the positively charged K134 side chain (Figure 2c). The ligand carboxylate is also hydrogen bonded to the N atom of I137. The rest of the PBA molecule extends upside down relative to the orientation of the ligand in the lowest-energy cluster with R240 binding. Indeed, the ring makes vdW interactions with F112, A135, and T130. When bound to K134, the ligand methylene C atom, Gly-Cα-like, is positioned ~10 Å from the catalytic Cu_M center. This large distance suggests that this orientation is "nonproductive" in terms of "suicide" inhibition.

Various PBA derivatives were studied by docking analysis. Among all the compounds experimentally tested for inhibition, we chose to undertake calculations for five compounds representative of two classes of inhibitors: two high-activity compounds (**2a** and **2d**) and three low-activity compounds (POBA, **1**, and **3**).

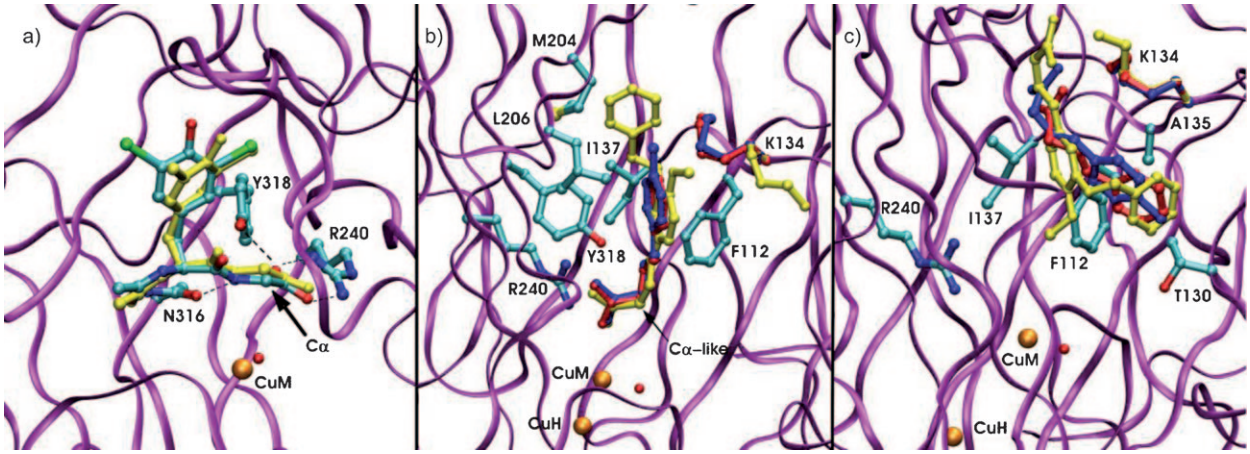

Figure 2. a) Superposition of co-crystallized (cyan) and docked (yellow) IYG in complex with PHM (magenta ribbon). Protein residues interacting with IYG are represented in ball-and-stick mode; the Cu_M atom and a ligated water molecule are represented as orange and red spheres, respectively. The Cα atom of Gly is indicated by the arrow. b) Representative conformations of the lowest-energy and most populated clusters (characterized by the COO^-/R240 interaction) obtained for PBA (red), **2a** (dark blue), and **2d** (yellow) ligands. c) Representative conformations of the most significant clusters characterized by the COO^-/K134 interaction for PBA (red), **2a** (dark blue), and **2d** (yellow) ligands. Corresponding conformations of the flexible K134 side chain are highlighted in the same color as the respective ligand. Relevant residues lining the binding pockets are represented in ball-and-stick mode; Cu atoms are represented as orange spheres.

 © 2010 Wiley-VCH Verlag GmbH & Co. KGaA, Weinheim

The docking calculations with **2a** and **2d** again resulted in two main binding modes characterized by either the COO^-/R240 or the COO^-/K134 interaction. As with PBA docking, the lowest-energy cluster conformation is the one with the COO^-/R240 interaction (Figure 2b). For both inhibitors, the best-docked compound shows an orientation similar to the lowest-energy conformation of PBA (Figure 2b), thus positioning the Gly-Cα-like atom ~5–6 Å from the Cu_M center. In **2a**, the methyl group attached to the ring at the *para* position interacts with Cδ2 of L206 and Cδ of K134 (~3.8 Å). On the other hand, the larger compound **2d** has additional stabilization from the second ring located in a hydrophobic pocket pushed deeper toward a β-sheet in one of the two domains. Specifically, the second ring of **2d** displays vdW interactions with M204, L206, and F331. Moreover, the O atom between the two six-membered rings establishes a hydrogen bond with the I137 amido group. The large number of stabilizing interactions is responsible for the high affinity of ligand **2d** for PHM. The estimated K_i values for compounds **2a** and **2d** are 28.9 and 4.1 μM, respectively (Table 1).

The COO^-/K134 binding mode is higher in energy than the COO^-/R240 mode for both **2a** and **2d** compounds. In the case of **2a**, the COO^-/K134 binding mode exhibits a molecular orientation analogous to that already observed and described for the COO^-/K134 cluster of PBA (Figure 2c). A similar result was found for compound **2d**, where the position of the first ring (the most distal from the COO^- group) is stabilized by vdW interactions with A135, T130, and C131 (Figure 2c). The second ring, instead, adopts a position close to that found for the COO^-/R240 cluster of PBA. In the COO^-/K134 cluster conformations, the Gly-Cα-like atoms are ~9–10 Å away from the Cu_M center.

We analyzed three other PBA derivatives by molecular docking, namely **3**, POBA, and **1**, for which assay data indicate low inhibitor activity (131, 440, and 700 μM, respectively). As far as compound **3** is concerned, docking calculations were carried out on both enantiomers (1*R*,2*S*)-**3** and (1*S*,2*R*)-**3**, but only (1*S*,2*R*)-**3** is discussed, given the similarity of the results. It turns out that for all the three poor inhibitors, the best-docked solutions (the most populated and the lowest-energy clusters) exhibit interactions with K134 instead of R240 (Table 1 herein and table 1 in the Supporting Information). Therefore, molecules experimentally proven to be weak inhibitors prefer the "unproductive" mode, which places the Gly-Cα-like atom too far away from Cu_M. In particular, the preferred binding modes of POBA, **1**, and **3** are depicted in Figure 3.

For compound **3** and POBA, the six-membered ring occupies the previously described hydrophobic pocket with an orientation similar to that found for the COO^-/R240 cluster of **2a** and PBA. In the case of compound **3**, the three-membered ring makes vdW interactions with M204, I137, and L206, thus partially occupying the enlarged pocket explored by compound **2d** in the COO^-/R240 binding mode. For the POBA ligand, the carbonyl group interacts with the amido group of I137. The lowest-energy conformation of **1** is superimposable with the COO^-/K134 cluster of PBA, apart from the second six-membered ring, which makes vdW contacts with Y318. Notably,

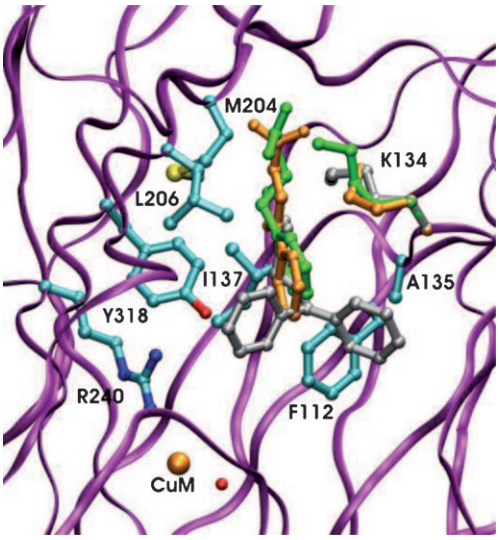

Figure 3. Representative conformations of the preferred binding modes for POBA (orange), **1** (grey), and **3** (green) ligands. Corresponding conformations of the flexible K134 side chain are highlighted in the same color of their respective ligands. Relevant residues lining the binding pockets are represented in ball-and-stick mode; the Cu_M atom and a ligated water molecule are represented as orange and red spheres, respectively.

docking calculations for PBA and its derivatives often show the presence of a cluster of high-energy conformations exhibiting hydrophobic rings or moieties which extend into the inter-domain crevice, close to the Cu_H center. The rings are frequently sandwiched between P271 and H107, while the COO^- tail often maintains the electrostatic interaction with R240.

Discussion

New PHM inhibitors derived from PBA were designed, synthesized, and tested through both experimental and theoretical approaches. Whereas compounds **1** and **3** exhibit poor efficiency in PHM inhibition, interesting results emerged for compounds **2a**–**d**. These compounds behave as mechanism-based inhibitors, with K_i values in the range from 3.9 to 20 μM. Among them, compound **2d**, which bears a *para*-benzyloxy substituent, exhibits better inhibition features ($K_i = 3.9$ μM, $k_{inact}/K_i = 427\ M^{-1}s^{-1}$) than the parent compound PBA ($K_i =$ 19 μM, $k_{inact}/K_i = 82\ M^{-1}s^{-1}$). We demonstrated that it is possible to increase the affinity of PBA derivatives for PHM by appropriate functionalization of the aromatic nucleus.

A docking study of these new PHM inhibitors was carried out to assess their putative binding mode with PHM and to explore the details of the environmental and structural features in the vicinity of the active site. Two main binding modes of the analyzed inhibitors were detected, characterized by different anchoring points for the ligand carboxylate, i.e., the positively charged side chains of either K134 or R204. Given these key interactions, the two inhibitor binding modes are referred to as COO^-/R240 and COO^-/K134 (Scheme 4). In both binding modes, the aromatic ring moieties are located in a hydrophobic cavity that is different from the pocket accommodating the

 © 2010 Wiley-VCH Verlag GmbH & Co. KGaA, Weinheim

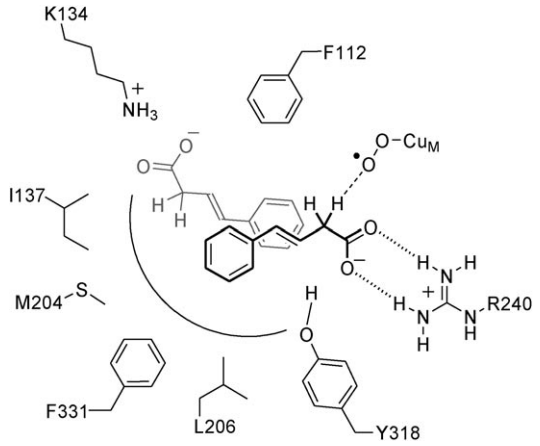

Scheme 4. Productive (black) versus unproductive (grey) binding modes for PBA derivatives.

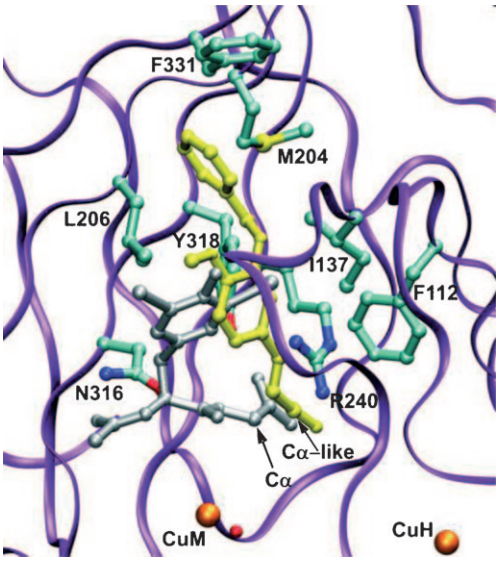

Figure 4. Binding pocket conformations for crystallographic IYG (grey) and **2d** (yellow).

diiodotyrosyl moiety of IYG in the crystal structure (Figure 4).[3,4] Indeed, this cavity consists of several hydrophobic residues: Y318, F112, I137, and L206. Moreover, large ligands such as compound **2d** are extended in the hydrophobic pocket, displaying additional vdW interactions with M204 and F331.

Interestingly, our results indicate that inhibitors which prefer the COO^-/R240 binding mode (PBA and **2a–d**) are those that show the best suicide inhibition features. On the other hand, ligands that prefer the COO^-/K134 mode (POBA, **1**, and **3**) are those that have poor suicide inhibition features.

As suggested by experimental data for these inhibitors, the COO^-/R240 binding mode is consistent with the suicide mechanism involving hydrogen atom abstraction by the copper–oxygen species and formation of a delocalized radical. Indeed, this binding mode places the Gly-Cα-like atom ~6 Å from the Cu_M center (Figure 4). A certain freedom of movement within the binding pocket is reasonable,[1] and can account for a shorter distance between the hydrogen (on the Cα-like atom) to be abstracted and the oxygen-activated species ligated to Cu_M. Hence, this binding mode can be considered "productive" in terms of processing these compounds as substrates. On the other hand, the COO^-/K134 mode places the inhibitor Gly-Cα-like atom too far away from Cu_M, resulting in an "unproductive" mode.

Although docking calculations provide insight into the inhibitor binding mode in agreement with experimental data, they are unable to reproduce accurate K_i values. Inspection of Table 1 reveals that a rather good agreement between experimental and theoretical K_i values is achieved only in the case of compounds **2a**, **2d**, and PBA, whereas poor agreement is observed for compounds **1** and **3**.

Even though the COO^-/R240 electrostatic interaction turned out to be the critical one for effective inhibitor activity, the presence of K134 interactions highlighted by the docking results are also of interest. This Lys residue, located at the mouth of the inter-domain crevice near the active site, may serve as a strong attractor for a negatively charged moiety diffusing from the external protein surface to the substrate-binding site. This region might be a peripheral binding site to be fruitfully explored in the design of novel high-affinity and selective inhibitors. Indeed, K134 is a conserved residue in mammalian PHM enzymes, whereas it is not found in sequences from other sources.

The PHM inhibition mechanism by PBA is still under debate. Unlike other mechanism-based inhibitors, inhibition by PBA does not imply a covalent binding of inhibitor to PHM, as no PHM-containing radioactivity was observed with the use of [^{3}H]PBA as inhibitor.[15] However, the formation of a PBA allylic radical has been proposed to occur during the inhibition process (Scheme 2).[15] It has been speculated that this resonating radical can dissociate from the enzyme prior to hydroxylation, thus leaving an activated copper–oxygen species, and this mechanism is responsible for autoxidation.[15] This inactivation pathway has already been proposed for other inhibitors.[26,27] However, another possible explanation is suggested by the docking calculations, which highlight an interaction between PBA and the Y318 residue (Figure 5). In the COO^-/R240 binding mode, docking results indicate that PBA Cα and Cγ atoms are ~3–4 Å from the Oζ atom of the Y318 residue. A hydrogen atom transfer from Y318 to the PBA radical could be responsible for the inactivation via the formation of an activated copper–hydroperoxo species and a tyrosinyl radical, both able to inactivate PHM. Notably, in dopamine β-hydroxylase (DβM; EC 1.14.7.1),[28] a copper-containing monooxygenase that has significant similarities to PHM,[29] the participation of Y278 (corresponding to Y318 in PHM) in enzyme inactivation was observed,[26,27] as well as the formation of a quinone on ascorbate-inactivated DβM.[30]

[1] *PHM-catalyzed hydroxylation of PBA that leads to α- and γ-hydroxy-PBA as mixture of enantiomers indicates a freedom of movement within the binding pocket (Scheme 2).*[15]

 © 2010 Wiley-VCH Verlag GmbH & Co. KGaA, Weinheim

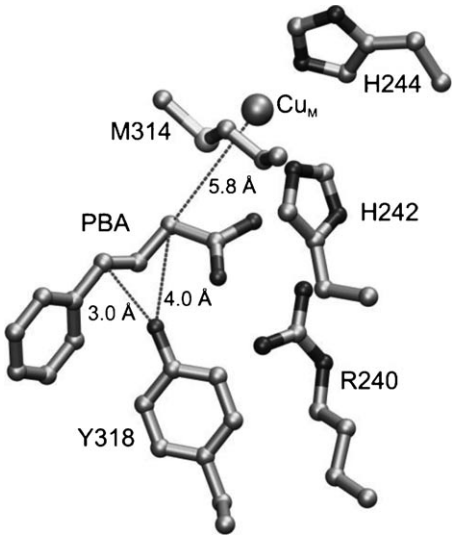

Figure 5. COO^-/K134 binding mode for the PBA molecule. PBA–Cu_M and PBA–Y318 distances on opposite sides of the pocket are shown.

Conclusions

We have designed, synthesized, and tested various PBA derivatives both in vitro and in silico, and have demonstrated that it is possible to increase their affinity for PHM through appropriate functionalization of the aromatic nucleus. Docking calculations underscored two different binding modes for PBA derivatives (productive versus unproductive), also giving hints on possible roles played by K134 and Y318 located close to the active site. These results will be useful for the design of new molecules with improved inhibition features against PHM. Along these lines, a promising starting point for the design of novel PHM inhibitors could be represented by compound **2d**, which is a high-affinity inhibitor, as shown by both experimental and theoretical studies.

Due to the key role played by α-amidated peptide hormones in various human diseases,[7] PHM still represents a potential target for drug design. Moreover, a new and interesting application of PHM inhibitors as effective insecticides with low toxicity toward humans has recently been suggested.[12] In this context, our structure–activity study could be useful for the rational design of more effective anti-PHM drugs with potential application in various fields.

Experimental Section

Chemistry

All reagents were obtained from commercial sources and were used as received. THF was distilled from sodium benzophenone. Silica gel TLC and column chromatography were performed with Merck Kieselgel 60 F_{254} and silica gel 60 (0.063–0.200 mesh). Elemental analyses (C, H, N, S) were measured with a Carlo Erba EA 1108 analyzer. NMR spectra were recorded with Bruker Avance DPX200 and DPX300 instruments using $(CH_3)_4Si$ as internal reference. X-ray analysis was performed on a Bruker–Nonius Kappa CCD.

4-(4-Benzyloxy)phenyl-3-butenoic acid (2c): A suspension of 4-benzyloxybenzaldehyde (2.30 g, 10.80 mmol, 1 equiv) and 2-carboxyethyltriphenylphosphonium bromide (4.5 g, 10.80 mmol, 1 equiv) in anhydrous THF (40 mL) was maintained under agitation at 0 °C. *t*BuOK (2.55 g, 22.68 mmol, 2.1 equiv) in anhydrous THF (25 mL) was then added dropwise over 20 min. The mixture was maintained under agitation at room temperature for 18 h. Ice-cold H_2O was then added (100 mL), and the mixture was extracted with Et_2O (3×100 mL). The aqueous phase was then acidified to pH 2 by the addition of concentrated HCl and washed with EtOAc (3× 80 mL). The organic phases were collected, washed with brine (10 mL), and dried over Na_2SO_4. Evaporation of the solvent under vacuum produced a crude orange oil, which was recrystallized in CH_3CN. Recrystallization afforded compound **2c** as a pale-yellow solid (1.40 g, 5.18 mmol, 48%): mp: 95–96 °C; ^{1}H NMR (300 MHz, CD_3OD): $\delta = 3.22$ (d, $J = 6.9$ Hz, 2H), 5.10 (s, 2H), 6.21 (dt, $J = 15.9$ and 6.9 Hz, 1H), 6.48 (d, $J = 15.9$ Hz, 1H), 6.85 (d, $J = 8.4$ Hz, 2H), 7.31–7.48 ppm (m, 7H); ^{13}C NMR (75 MHz, $CDCl_3$): $\delta = 39.86$ (CH_2), 71.88 (CH_2), 116.84 (2CH), 122.03 (CH), 129.31 (2CH), 129.43 (2CH), 129.75 (CH), 130.38 (2CH), 132.41 (C), 134.61 (CH), 139.59 (C), 160.66 (C), 168.33 ppm (C); Anal. calcd for $C_{17}H_{16}O_3$: C 76.10, H 6.01, found: C 76.12, H 5.99.

4-(3-Benzyloxy-4-methoxy)phenyl-3-butenoic acid (2d): The title compound was prepared from 3-benzyloxy-4-methoxybenzaldehyde (2.33 g, 9.6 mmol, 1 equiv), 2-carboxyethyltriphenylphosphonium bromide (4 g, 9.6 mmol, 1 equiv) and *t*BuOK (2.27 g, 20.16 mmol, 2.1 equiv) in anhydrous THF (40 mL) using the procedure described above for the preparation of **2c**. Recrystallization of the crude orange oil afforded compound **2d** as a pale-yellow solid (1.05 g, 3.46 mmol, 40%): mp: 110–112 °C; ^{1}H NMR (300 MHz, CD_3OD): $\delta = 3.22$ (d, $J = 6.9$ Hz, 2H), 3.87 (s, 3H), 5.13 (s, 2H), 6.17 (dt, $J = 15.9$ and 6.9 Hz, 1H), 6.44 (d, $J = 15.9$ Hz, 1H), 6.92–7.00 (m, 2H), 7.10 (s, 1H), 7.31–7.50 ppm (m, 5H); ^{13}C NMR (75 MHz, $CDCl_3$): $\delta = 39.75$ (CH_2), 57.42 (CH_3), 73.12 (CH_2), 114.15 (CH), 114.20 (CH), 122.09 (CH), 122.29 (CH), 129.67 (2CH), 129.80 (CH), 130.33 (2CH), 132.71 (C), 134.79 (CH), 139.60 (C), 150.47 (C), 151.78 (C), 176.65 ppm (C); Anal. calcd for $C_{18}H_{18}O_4$: C 72.47, H 6.08, found: C 72.44, H 6.09. Crystallographic data: $C_{18}H_{18}O_4$, $M_r = 298.32$ Da, monoclinic, colorless crystal ($0.4 \times 0.25 \times 0.2$ mm^3), $a = 14.429(2)$ Å, $b = 13.913(4)$ Å, $c = 7.867(5)$ Å, $\beta = 97.175(1)°$, $V = 784.31(1)$ Å^3, space group: $P2_1/c$, $Z = 4$, $\rho = 1.27$ g cm^{-3}, $\mu(MoK_\alpha) = 0.89$ cm^{-1}, 3847 unique reflections in the 2.99–30.47 θ range, 199 parameters refined on F^2 [Shelxl] to final indices $R[F^2 > 4\sigma(F^2)] = 0.064$ (2665 reflections), $wR50$ ($w = 1/[\sigma 2(Fo^2) + (0.0585P)^2 + 0.5685P]$ for which $P = (F_o^2 + 2F_c^2)/3) = 0.164$ (all reflections). The last residual Fourier-positive and -negative peaks were equal to 0.168 and −0.169, respectively. CCDC 735325 (**2d**) contains the supplementary crystallographic data for this paper. These data can be obtained free of charge from The Cambridge Crystallographic Data Centre via www.ccdc.cam.ac.uk/data_request/cif.

Enzymology

PAM preparation and enzyme assays

For all enzymatic studies, we used the membrane-bound form of porcine PAM prepared according to a procedure described for the rat PAM form.[14] The source was the pig left atrial membrane. In a typical procedure, 50 g atrial tissue gives membrane-bound PAM with a specific activity of 1.4 nmol min^{-1} (mg enzyme)$^{-1}$.

PHM activity was assayed at 37 °C in a total volume of 500 μL MES buffer (pH 6.5, 100 μM) containing NEM (500 μM), $CuSO_4$ (2 μM), as-

 © 2010 Wiley-VCH Verlag GmbH & Co. KGaA, Weinheim

corbic acid (10 mM), catalase (6500 U; Sigma Chemical Co.), and *N*-dansyl-D-Tyr-L-Val-Gly (200 μM). Kinetics analyses were performed at 37 °C using a minimum of five concentrations in triplicate. Enzyme dilutions were adjusted so that maximum conversion of substrate to product remained within the linear range of the assay (< 20%). Reactions were stopped by the addition of perchloric acid (20 μL). After centrifugation (15000 rpm, 15 min), the supernatant was quenched by the addition of 65 μL of a solution of 2 M NaOH containing EDTA (50 μM). This final step is to ensure the total transformation of hydroxyglycine into amido compound and glyoxylic acid; 20 μL of this solution is then analyzed by reversed-phase (RP) HPLC. Chromatography was performed using a C_{18} column (Lichrospher® 100, RP18 5 μm, Agilent Technologies) on a Hewlett–Packard series 1100 HPLC system equipped with HP ChemStation software and a diode array detector. The system was operated at a flow rate of 1 mL min^{-1}, and a column temperature of 25 °C under isocratic conditions with 30% CH_3CN in acetate buffer (pH 6.5, 100 mM) as the mobile phase. Elution profiles were monitored at λ 250 nm. Under these conditions the retention times were 3.6 min for *N*-dansyl-D-Tyr-L-Val-Gly and 6.5 min for *N*-dansyl-D-Tyr-L-Val-NH_2.

Inhibition assays

Time-dependent PHM inactivation was assayed at 37 °C in a total volume of 500 μL MES buffer (pH 6.5, 100 mM) containing NEM (500 mM), $CuSO_4$ (2 μM), ascorbic acid (10 mM), catalase (6500 U; Sigma Chemical Co.), and inhibitor at various concentrations (0–10 μM). Reactions were initiated by the addition of enzyme. Aliquots (50 μL) were withdrawn at intervals of 1–20 min from the pre-incubation mixture and diluted into 450 μL assay solution of MES buffer (pH 6.5, 100 μM) containing NEM (500 μM), $CuSO_4$ (2 μM), catalase (6500 U), ascorbate (10 mM), and *N*-dansyl-D-Tyr-L-Val-Gly (200 μM). The enzyme reactions were analyzed by RP HPLC as described for the enzymatic assays above.

Docking calculations

The AutoDock (v. 4.0) software package[25] was chosen for docking the designed compounds into the PHM active site. The atomic coordinates of rat PHM oxidized form in complex with the ligand IYG were used in the calculations (PDB ID: 1OPM[3]). Although experimental inhibition tests were performed on pig PHM, molecular docking studies were carried out with the crystal structure from rat PHM, the only form available in the RCSB Protein Data Bank. Notably, the sequences of the catalytic cores for all available mammalian PHMs are highly conserved. Moreover, all residues within the hydrophobic pocket discussed herein and found to be relevant for the binding of PBA derivatives and their involvement in the mechanism-based inhibition of PHM (F112, K134, I137, M204, L206, R240, N316, Y318, and F331; Scheme 4) are strictly conserved across the 57 species and mammalian PHM isoforms (see figures 7 and 8 in the Supporting Information).

Amber charges and polar hydrogen atoms were added to the protein by using the PDB2PQR server [http://pdb2pqr-1.wustl.edu/pdb2pqr/ (accessed July 8, 2010)]. To compensate for overestimation of the electrostatic contribution of the copper ion we established its charge to +0.8 according to Hu and Shelver[31] and our previous tests. Ligand coordinates were generated by the *builder* module of the Insight software package, whereas charges were computed by means of semiempirical MNDO calculations. Ligand-active torsions were defined by the AutoTors tool of the AutoDock package. Affinity grids with dimensions 70×70×70 points (with a spacing of 0.33 Å) were built around the binding site, based on the location of the co-crystallized ligand, providing enough space for translational and rotational freedom of the ligands. The van der Waals parameters for copper ($\varepsilon = 0.012$ kJ mol^{-1}, $\sigma = 1.26$ Å) were chosen according to Cecconi et al.[32]

The Lamarckian genetic algorithm (LGA) and the pseudo-Solis and Wets methods were used for the conformational search. The maximum number of energy evaluations was set to 2.5×10^7, and a maximum number of 2.7×10^5 genetic algorithm operations were generated on a single population of 150 individuals. Operator weights for crossover, mutation, and elitism were default parameters, 0.80, 0.02, and 1, respectively; 100 runs were performed. The resulting docked conformations of the ligand were clustered and ranked according to the default AutoDock scoring function using an RMSD of 3.0 Å. Calculations for representative ligands (IYG and PBA derivatives) were also carried out by using the reduced rat PHM structure (PDB ID: 1SDW[4]) in order to verify that similar results (data not shown) were obtained by starting from a different redox state of the protein. In this case, the charge on the Cu atoms was decreased to +0.3, according to the literature.[33]

Acknowledgements

The authors thank Dr. Patrick Slama for discussions, Mr. Luca De Luca for technical assistance, and Dr. Charles Danzin for PhD financial support (S.P.). This work was supported by a bilateral CNR/CNRS agreement.

Keywords: 4-phenyl-3-butenoic acid · computer chemistry · docking · inhibitors · monooxygenases

[1] S. T. Prigge, R. E. Mains, B. A. Eipper, L. M. Amzel, *Cell. Mol. Life Sci.* **2000**, *57*, 1236–1259.
[2] S. T. Prigge, A. S. Kolhekar, B. A. Eipper, R. E. Mains, L. M. Amzel, *Science* **1997**, *278*, 1300–1305.
[3] S. T. Prigge, A. S. Kolhekar, B. A. Eipper, R. E. Mains, L. M. Amzel, *Nat. Struct. Biol.* **1999**, *6*, 976–983.
[4] S. T. Prigge, B. A. Eipper, R. E. Mains, L. M. Amzel, *Science* **2004**, *304*, 864–867.
[5] X. Siebert, B. A. Eipper, R. E. Mains, S. T. Prigge, N. J. Blackburn, L. M. Amzel, *Biophys. J.* **2005**, *89*, 3312–3319.
[6] F. N. Bolkenius, A. J. Ganzhorn, *Gen. Pharmacol.* **1998**, *31*, 655–659.
[7] J. P. Hinson, S. Kapas, D. M. Smith, *Endocr. Rev.* **2000**, *21*, 138–167.
[8] P. Rocchi, F. Boudouresque, A. J. Zamora, X. Muracciole, E. Le Chevalier, P.-M. Martin, L. Ouafik, *Cancer Res.* **2001**, *61*, 1196–1206.
[9] P.-M. Martin, L. Ouafik, Patent WO02066492, 2002.
[10] M. A. García, S. Martín-Santamaría, B. de Pascual-Teresa, A. Ramos, M. Julián, A. Martínez, *Expert Opin. Ther. Targets* **2006**, *10*, 1–15.
[11] M. D. Andrews, K. A. O'Callaghan, J. C. Vederas, *Tetrahedron* **1997**, *53*, 8895–8906.
[12] D. J. Merkler, A. S. Asser, L. E. Baumgart, N. Carballo, S. E. Carpenter, G. H. Chew, C. C. Cosner, J. Dusi, L. C. Galloway, A. B. Lowe, E. W. Lowe, Jr., L. King III, R. D. Kendig, P. C. Kline, R. Malka, K. A. Merkler, N. R. McIntyre, M. Romero, B. J. Wilcox, T. C. Owen, *Bioorg. Med. Chem.* **2008**, *16*, 10061–10074.
[13] A. Y. Jeng, R. A. Fujimoto, M. Chou, J. Tan, M. D. Erion, *J. Biol. Chem.* **1997**, *272*, 14666–14671.
[14] F. N. Bolkenius, A. J. Ganzhorn, M.-C. Chalnal, C. Danzin, *Biochem. Pharmacol.* **1997**, *53*, 1695–1702.
[15] W. J. Driscoll, S. Konig, H. M. Fales, L. K. Pannell, B. A. Eipper, G. P. Mueller, *Biochemistry* **2000**, *39*, 8007–8016.
[16] G. P. Mueller, W. J. Driscoll, B. A. Eipper, *J. Pharmacol. Exp. Ther.* **1999**, *290*, 1331–1336.

 © 2010 Wiley-VCH Verlag GmbH & Co. KGaA, Weinheim

[17] C. Walsh, T. Cromartie, P. Mariotte, R. Spencer, *Methods Enzymol.* **1978**, *53*, 437 – 448.
[18] S. G. Waley, *Biochem. J.* **1980**, *185*, 771 – 773.
[19] W. J. Johnson, J. W. Petersen, W. P. Schneider, *J. Am. Chem. Soc.* **1947**, *69*, 74 – 79.
[20] F. Ozaki, M. Matsukura, Y. Kabasawa, K. Ishibashi, M. Ikemori, S. Hamano, N. Minami, *Chem. Pharm. Bull.* **1992**, *40*, 2735 – 2740.
[21] S. R. Nagarajan, H.-F. Lu, A. F. Gasiecki, I. K. Khanna, M. D. Parikh, B. N. Desai, T. E. Rogers, M. Clare, B. B. Chen, M. A. Russell, J. L. Keene, T. Duffin, V. W. Engleman, M. B. Finn, S. K. Freeman, J. A. Klover, G. A. Nickols, M. A. Nickols, K. E. Shannon, C. A. Steininger, W. F. Westlin, M. M. Westlina, M. L. Williams, *Bioorg. Med. Chem.* **2007**, *15*, 3390 – 3412.
[22] H. E. Simmons, R. D. Smith, *J. Am. Chem. Soc.* **1959**, *81*, 4256 – 4264.
[23] A. G. Katopodis, S. W. May, *Biochemistry* **1990**, *29*, 4541 – 4548.
[24] R. Kitz, I. B. Wilson, *J. Biol. Chem.* **1962**, *237*, 3245 – 3249.
[25] G. M. Morris, D. S. Goodsell, R. S. Halliday, R. Huey, W. E. Hart, R. K. Belew, A. J. Olson, *J. Comput. Chem.* **1998**, *19*, 1639 – 1662.
[26] W. E. Dewolf, S. A. Carr, A. Varrichio, P. J. Goodhart, M. A. Mentzer, G. D. Roberts, C. Southan, R. E. Dolle, L. I. Kruse, *Biochemistry* **1988**, *27*, 9093 – 9101.
[27] G. K. Farrington, A. Kumar, J. J. Villafranca, *J. Biol. Chem.* **1990**, *265*, 1036 – 1040.
[28] L. C. Stewart, J. P. Klinman, *Annu. Rev. Biochem.* **1988**, *57*, 551 – 592.
[29] J. P. Klinman, *J. Biol. Chem.* **2006**, *281*, 3013 – 3016.
[30] P. Slama, F. Jabre, T. Tron, M. Réglier, *FEBS Lett.* **2001**, *491*, 55 – 58.
[31] X. Hu, W. H. Shelver, *J. Mol. Catal. B* **2003**, *22*, 115 – 126.
[32] I. Cecconi, A. Scaloni, G. Rastelli, M. Moroni, P. G. Vilardo, L. Costantino, M. Cappiello, D. Garland, D. Carper, J. M. Petrash, A. Del Corso, U. Mura, *J. Biol. Chem.* **2002**, *277*, 42017 – 42027.
[33] A. de La Lande, S. Marti, O. Parisel, V. Moliner, *J. Am. Chem. Soc.* **2007**, *129*, 11 700 – 11 707.

Received: May 17, 2010
Revised: June 30, 2010
Published online on August 16, 2010

 © 2010 Wiley-VCH Verlag GmbH & Co. KGaA, Weinheim